Investigation of waste PCB leach residue as a reducing agent in smelting processes

Desmond Attah-Kyei[a,b,*], Guven Akdogan[a], Christie Dorfling[a], Johan Zietsman[c],
Daniel Lindberg[b,d], Fiseha Tesfaye[d], Quinn Reynolds[e]

[a] Department of Process Engineering, Stellenbosch University, Private Bag X1, Matieland 7602, South Africa
[b] Aalto University, Department of Chemical and Metallurgical Engineering, Kemistintie 1, 02150 Espoo, Finland
[c] Ex Mente Pty (Ltd), Pretoria, PO Box 10214, Centurion 0046, South Africa
[d] Åbo Akademi University, Johan Gadolin Process Chemistry Centre, Piispankatu 8, FI-20500 Turku, Finland
[e] Pyromet Division, Mintek, 200 Malibongwe Drive, Private Bag X3015, Randburg 2125, South Africa

ABSTRACT

The advancement in technology has resulted in the development of newer and improved electrical products. The older products are becoming obsolete and are discarded as waste at a continuously increasing trend. Printed circuit board (PCB) is the main focus of electronic waste recycling because of the inherently high value of contained metals such as gold and copper. Hydrometallurgical route, which is often used to recover the metals, does not take into account the non-metallic PCB fractions. These non-metallic fractions may end up in landfills or incinerated which leads to secondary pollution. In this work, the use of the leached PCB waste fraction as reductant in primary metal smelting operations and solid state reduction is investigated.

Laboratory-scale experiments and thermodynamic modelling were performed to simulate solid state reduction of hematite (Fe_2O_3) using various blends of PCB and graphitic carbon. Differential Scanning Calorimeter (DSC) analysis of several samples were performed up to 1200 °C. Thermodynamic modelling was done using FactSage to predict the products of the hematite reduction below 1600 °C. The study showed that PCB residue might be used to partially replace the conventional reductants. The investigations revealed that at temperatures below 1000 °C, PCB reduces hematite to lower forms of iron oxide at a faster rate than that of graphite. The optimal blend contains about 20 wt% PCB residue which has the same reduction degree as graphite.

Thermodynamic modelling of iron smelting was also performed using various blends of PCB and coal. The models showed that PCB residue might be used to partially replace the conventional reductants. The study revealed that in iron smelting, the optimal blend contains around 20 wt% PCB residue, with energy savings of 150 kWh/t of ore to achieve the same metal recovery.

1. Introduction

Due to the rapid growth of the production of electrical and electronic equipment (EEE), there has been an increase in the worldwide generation of Waste Electric and Electronic Equipment (WEEE). This increase is as a result of the advancement of technology and in some circumstances, the high cost of repairing equipment in comparison to buying new equipment.

Recently, it has been estimated that the world generates about 45.4 million tonnes of WEEE each year and the amounts are expected to increase by about 3–5% annually (Cucchiella et al., 2015; Tesfaye et al., 2017). The disposal of electronic wasted via landfilling is destructive to the environment because of the presence of high content of heavy metals and brominated flame retardants (BFR).

Printed circuit board (PCB) is the principal and essential part of electronic equipment since it electrically connects and mechanically supports the other electronic components such as resistors, capacitors and integrated circuits. It is found virtually in all electronic products (Duan et al., 2011). The basic structure of the PCB is the copper-clad laminate consisting of glass-reinforced epoxy resin and a number of metallic materials including base and precious metals (Ghosh et al., 2015). Cui and Anderson, (2016) reported that PCBs contain more base and precious metals than their respective ore and that the gold content in PCBs is 35–50 times higher than gold ore. As a result of its high concentration, e-waste recycling, and metal recovery is an attractive prospect from economic, technical and environmental points of view.

Zheng et al. (2009) classified PCB recycling into three branches according to the different material recovering processes; physical, thermal and chemical processing. In physical processing, the PCB is crushed and the metallic components are separated from the non-metallic fractions based on their densities, magnetic properties, and electric conductivities (Yamane et al., 2011; Yoo et al., 2009). Thermal processing involves the use of incineration in order to recover the metals or as part of the combustion of municipal solid waste (MSW). This method is available and very simple. Metal making industries such as Noranda (Quebec, Canada) and Boliden Rönnskär (Sweden) recover valuable metals from electronic waste using pyrometallurgical processes (Tesfaye et al., 2017). In the chemical recycling process, PCB is treated using hydrometallurgical techniques. It consists mainly of leaching, purification, and recovery of metals. The constituents of PCB are dissolved to form a pregnant solution using a suitable lixiviant such as sulphuric acid, cyanide, thiosulphate, halides. The metallic fraction is leached from the PCB. Hydrometallurgy is preferred because it is accurate, highly predictable and easily controlled. Hydrometallurgical treatment of e-waste has been found to be more efficient and environmentally friendly than other recovery processes, such as physical separation (Cui and Anderson, 2016; Diaz et al., 2016; Sohaili et al., 2012). However, the shortcoming of this process is that it does not consider the non-metallic fractions which forms about 60% of the PCB (Ogunniyi et al., 2009; Shuey and Taylor, 2005). From an environmental management perspective, a zero-waste approach of recycling should be developed to gain value from and reduce the environmental impact of both the metallic and non-metallic fractions of the PCB waste.

There are several ways of recycling the non-metallic fractions of PCB. Bazargan et al. (2014) studied the recovery of high purity silica from non-metallic component of PCB using thermal treatment. Their results revealed the possibility of getting 99% pure SiO_2 of specific surface area (BET) as high as 300 m^2/g. Recycling of polymeric compounds are generally classified as material recycling, chemicals recycling, or energy recovery through combustion (Fink, 1999; Fisher et al., 2005). Material recycling approaches refer to applications where the non-metallic fractions of the PCBs are used as inclusions or fillers in concrete, asphalt materials, or thermoplastic, resin, or similar matrix composites with minimal processing. Chemical recycling, on the other hand, refers to processes in which chemicals and fuels are produced from PCB leach residue using techniques such as pyrolysis, supercritical fluids depolymerisation or hydrogenolytic degradation.

While material recycling is promising, it has found only limited industrial applications due to the diverse composition of circuit boards, poor compatibility between the non-metallic fractions and matrix materials, potential leaching of residual hazardous metals, and generally low public acceptance of products containing recycled PCBs. The high costs associated with chemical recycling methods, on the other hand, often deter the adoption of these processes even though it is the most effective method to manage hazardous components and to fully utilise all elements (Guo et al., 2009).

Due to the complex composition of PCB, recovery by thermal treatment is likely to be the most feasible process route from a technical and economic standpoint. In this study, the feasibility of using the non-metallic PCB fractions as a reductant in pyrometallurgical unit operations was investigated. Several authors have investigated the recycling of plastics as feedstock for reductive smelting operations. One of the major applications in this field involves the use of polymer waste in blast furnaces for steelmaking, where plastics are substituted for coke, coal, or oil used for ore reduction and heating. NKK Keihnn Works in Japan first implemented this technology after it was developed by Bremen Steelworks in Germany (Zie and Stanek, 2001).

Some factors that influence the amount of polymer waste that can be added to blast furnace feeds include the carbon to hydrogen ratio, the energy content, supply rates required to sustain continuous operation, as well as the chloride and the residual non-ferrous metal content of the waste (Fink, 1999; Nourreddine, 2007).

The use of polymer waste to replace conventional reducing agents provide a number of advantages. The coal resources are conserved since there is a lower consumption of both coke and pulverized coal and there is a reduction in polymer waste being landfilled or incinerated. Moreover, energy resources are saved when plastics are used as reductants. This is because plastics have higher hydrogen to carbon ratio than coal. (Carpenter, 2010) stated that hydrogen is a more favourable reducing agent than carbon since the regeneration of hydrogen is faster and less endothermic than carbon monoxide regeneration and estimated that about 47 GJ/t is saved when plastic waste is used as reductants in blast furnaces.

The drawback in the use of the non-metallic fraction of PCB as reductant is the emission of toxic gases. However, Nourreddine (2007) and Zie and Stanek (2001) reported that the formation of dioxins is not problematic in these processing routes, but formation of bromine and chlorine containing gases such as HBr and HCl might result in corrosion of equipment (Fink, 1999; Hotta, 2003). The toxic gas emissions may be controlled by treating the off-gas or thermal decomposition at high temperatures (Stewart and Lemieux, 2003). Moreover, the use of polymer waste, and electronic scrap in particular, in metallurgical processes has been reported to lead to disturbances and contamination of products. Residual metals in the non-metallic fraction of the PCB waste might also affect the reduction process and metal quality; trace amounts of copper in steel, for example, results in a brittle product (Fink, 1999; Zie and Stanek, 2001).

2. Materials and methods

2.1. Pre-treatment and leaching of PCB

Discarded computers were partially dismantled by manually removing different components such as PCBs, batteries and the large components including stainless steel heat sinks, which are difficult to crush. The dismantled PCB was desoldered by submerging in 2 mol/dm^3 nitric acid for 24 h. The desoldered PCB was then cut into pieces of approximately 2 cm × 2 cm using a band saw and afterwards crushed using a hammer mill with the largest size passing a sieve of aperture 2 mm.

Leaching was performed using sulphuric acid and subsequently aqua regia at ambient temperature. 5 L of the acid was placed in a vessel and 500 g of the crushed PCB was added. Further leaching performed using aqua regia as lixiviant was to ensure that the metals are completely dissolved in the acid. Precious and base metals dissolved in the leachate can be recovered using techniques such as ion exchange or solvent extraction followed by electrowinning or precipitation (Correa et al., 2018; Cui and Zhang, 2008; Gurung et al., 2013). The residue was washed and air dried. About 35% of the mass of the PCB was lost during leaching (see Fig. 1).

2.2. Characteristics of PCB residue, coal and iron ore

Ultimate analysis (Table 1) and proximate analysis (Table 2) were performed on the PCB leach residue using Vario EL Cube Elemental and LECO CS 230 analysers, respectively. The ash content (Table 3) was analysed using induced couple plasma optical emission spectrometer (ICP-OES). Zeiss MERLIN Field Emission Scanning Electron Microscope (SEM) (Fig. 2) was used to observe the morphology of the PCB leached residue. In order to determine the composition of the residue, XRF analysis (Table 4) was performed on the PCB leach residue using PANalytical Axios Wavelength Dispersive spectrometer. XRF analysis was done to complement the ash analysis.

2.3. Reduction tests using differential scanning calorimetry (DSC) and thermogravimetry (TGA)

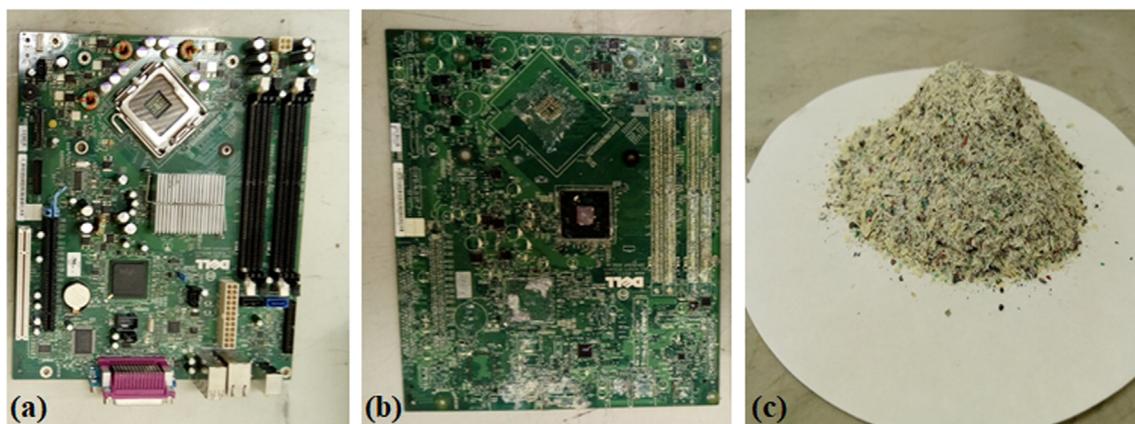Samples were prepared as shown in Table 7 by mixing high purity

Fig. 1. PCB obtained from discarded computers (a) before treatment, (b) after desoldering, and (c) after grinding.

Table 1
Ultimate analysis and halide determination of PCB leach residue (wt%).

C	H	N	S	O	F	Cl
28.5	3.06	1.10	0.54	23.1	0.25	0.42

Table 2
Proximate analysis (wt%) and calorific value (MJ/kg) of PCB leach residue.

Inherent moisture	Ash	Volatiles	Fixed carbon	Calorific value
3.60	40.10	44.80	11.50	12.08

(> 99%) hematite and graphite (99.99%) and PCB leached residue In order to understand the reduction process, thermo-gravimetric test were carried out in Netzsch STA 449 F1 Jupiter DSC-TGA coupled with Pfeiffer Vacuum ThermoStar GSD 301 T3 quadruple mass spectrometer (QMS).

About 20 mg of sample was weighed and placed in an alumina crucible and transferred to the DSC-TGA afterwards. The samples were heated from ambient temperature to 1200 °C at a heating rate of 10 °C /min. A constant flowrate of 70 ml/min Ar of purity (> 99.999%) was used. The QMS detected qualitatively the presence of CO, CO_2 and other gases predicted by FactSage© in the off gas. Hematite, graphite, PCB were placed individually in the DSC-TGA to understand the behaviour of each of the reagents at high temperatures under inert conditions. Reduction tests were subsequently carried out using the mixture of hematite and PCB-graphite blend. The products obtained after the reduction were analysed using SEM.

2.4. Thermodynamic simulation

Solid state reduction carried out in the DSC-TGA was simulated using FactSage 6.2 to predict the outcome of the reduction of hematite. 1 g of hematite was reduced with 0.532 g of reductant as used in the reduction tests. The FACT, ELEM, SGTE and FToxid databases were selected for the calculations. Thermodynamic calculations were performed up to 1600 °C with 25 °C interval at 1 atm. The compound species and the solution phases selected were, ideal gas, pure solids, Monoxide, Slag, Spinel, Liquid iron, BCC and, FCC.

Smelting of iron ore at 1700 °C was also performed using EMSIM, a

Fig. 2. Scanning electron microscope image of PCB residue.

Table 4
XRF results of PCB leach residue (wt%).

Al_2O_3	CaO	TiO_2	Fe_2O_3	K_2O
2.62	2.66	0.31	0.31	0.02
SiO_2	Na_2O	P_2O_5	MgO	L.O.I.
31.86	0.03	0.02	0.25	59.85

LOI = loss on ignition.

commercial web-based platform developed by Ex Mente Technologies (South Africa) for process modelling and simulation. In this work, EMSIM was used to create mass and energy balance models that were then used to evaluate the effect of varying PCB and coal in iron oxide smelting. In the EMSIM platform, 1 ton/h of iron ore (Table 6) was reduced with 300 kg/h of reducing agent consisting of different blends of coal (Table 5) and PCB. Tables 5 and 6 show the composition of coal (Anthracite 9 in Kleynhans et al., 2017) and iron ore (Mt. Newmann Concentrate (MNC) from Western Australia; Sohn and Fruehan, 2005) that were used in the simulation, respectively. Fig. 3 shows the flowsheet for the smelting operation which was simulated using EMSIM. It predicts the process behaviour and performance based on typical

Table 3
Ash analysis of PCB leach residue (wt%).

SiO_2	Al_2O_3	Fe_2O_3	TiO_2	CaO	MgO	Na_2O	K_2O	P	Ba	Cu
84.00	6.28	0.73	0.73	6.00	0.70	0.001	0.072	0.009	0.490	0.105

Table 5

Composition of coal (Kleynhans et al., 2017).

Carbon	Hydrogen	Nitrogen	Oxygen	Calorific value
80.10%	2.29%	1.45%	2.12%	30.49 MJ/kg
Moisture	**Ash**	**Volatiles**	**Fixed carbon**	**Sulphur**
1.60%	11.70%	5.10%	81.60%	0.74%

Table 6

Composition of Iron ore* used for smelting.

SiO$_2$	Al$_2$O$_3$	MgO	MnO	TiO	P$_2$O$_5$	K$_2$O	Fe
1.27	0.63	0.02	0.06	0.03	0.08	0.02	67.60

* Mt. Newmann Concentrate (MNC) from Western Australia (Sohn and Fruehan, 2005)

Table 7

Mass of hematite, PCB and graphite used in each reduction test.

Test	Mass (g) of		
	Hematite	PCB	Graphite
Hematite-graphite	1.0	0.0	0.532
Hematite-PCB	1.0	0.532	0.0
Hematite-20%PCB	1.0	0.1064	0.4256
Hematite-40%PCB	1.0	0.2128	0.3192
Hematite-80%PCB	1.0	0.4256	0.1064

operational inputs, similar to how the actual plant is operated. EMSIM relies on FactSage thermochemical data to model processes quickly and efficiently. The FactSage data makes it possible to estimate the enthalpies of input and output streams accurately, and therefore do accurate energy balance calculations (Zietsman et al., 2018).

3. Results and discussion

3.1. Thermal analysis of reagents

Hematite, graphite and PCB were placed individually in the DSC and heated to 1200 °C at 10 °C /min in argon atmosphere. Figs. 4–6

show the thermal behaviour of hematite, graphite and PCB under inert conditions.

Hematite alone was heated to 1200 °C as shown in Fig. 4. This was done to ascertain that the mass loss during hematite-reductant tests were solely due to removal of oxygen by the reducing agent and not hematite dissociation. Cao et al. (1997) reported that when hematite is heated in nitrogen atmosphere, it converted to magnetite. It is believed that only a negligible part of the hematite is converted to magnetite as shown in Eq. (1) since a peak was observed at about 800 °C but the mass loss was not significant.

$$3Fe_2O_3 \rightarrow 2Fe_3O_4 + 1/2\ O_2 \tag{1}$$
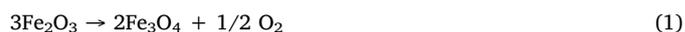
There were no significant change in mass when hematite only and graphite only were heated to 1200 °C. However, there was a notable loss of mass during the run with PCB only. About 45% of the PCB (Fig. 6) mass was lost between temperatures 100 °C and 350 °C. The mass loss is due to the pyrolysis of the PCB. The brominated epoxy resin is decomposed and volatilised. Several authors have observed similar results during their study of pyrolysis of PCB (Li et al., 2010; Rajagopal et al., 2016).

The off gas produced when PCB was heated to 1200 °C was analysed with the QMS and shown in Figs. 7 and 8. The presence of HBr, HS, S$_2$, H$_2$O and some hydrocarbons like CH$_4$ and C$_2$H$_6$ were detected in the off gas at that temperature. It should be noted that the QMS only detects qualitatively which species is present in the gas by showing a peak. The peaks cannot be compared to one another to determine the volume percentage of any substance at a specific temperature.

3.2. Hematite reduction in DSC-TGA

During the hematite-graphite reduction, the mass of the sample (Fig. 9) started to decrease around 900 °C. This indicates the onset of the reduction of hematite. It is believed that hematite is converted to magnetite at 900 °C, due to the change in mass and the release of CO$_2$. Jung and Yi (2013), in their study on the reduction of iron oxide with graphite attributed the initial formation of CO$_2$ as a combination of Eqs. (2) and (3). They stated that the gas–solid reaction (Eq. (3)) is faster than the solid–solid reaction (Eq. (2)). CO produced quickly reacts with hematite and produces CO$_2$. Thus only CO$_2$ is observed by the mass spectrometer.
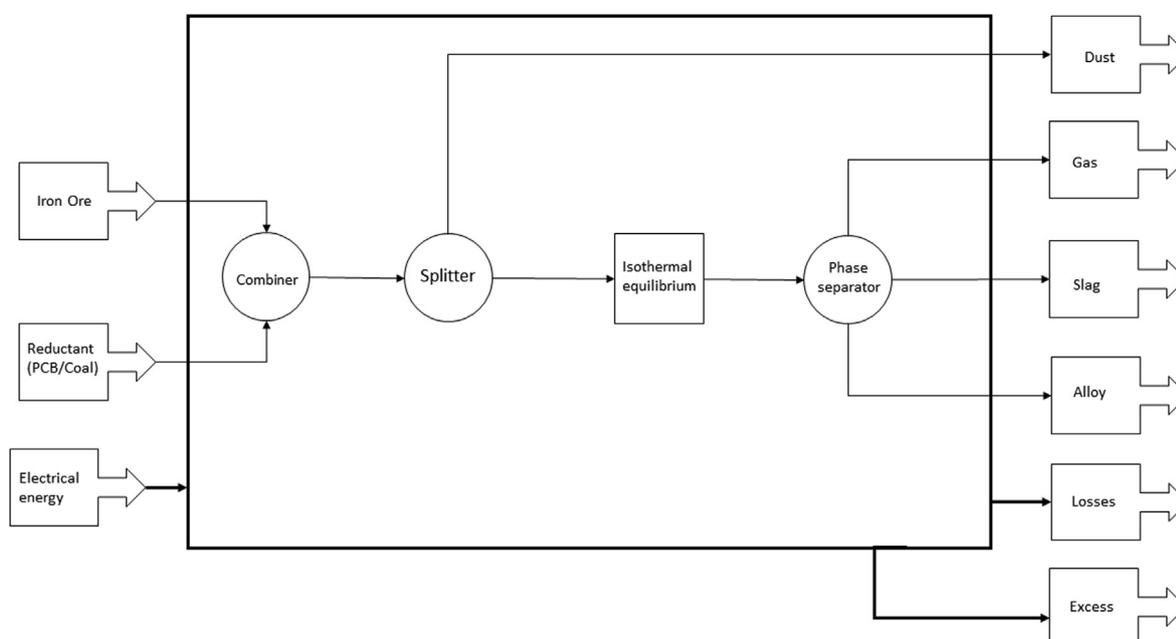

Fig. 3. Flowsheet for smelting operation simulated with the EMSIM software package of Ex Mente Technologies.
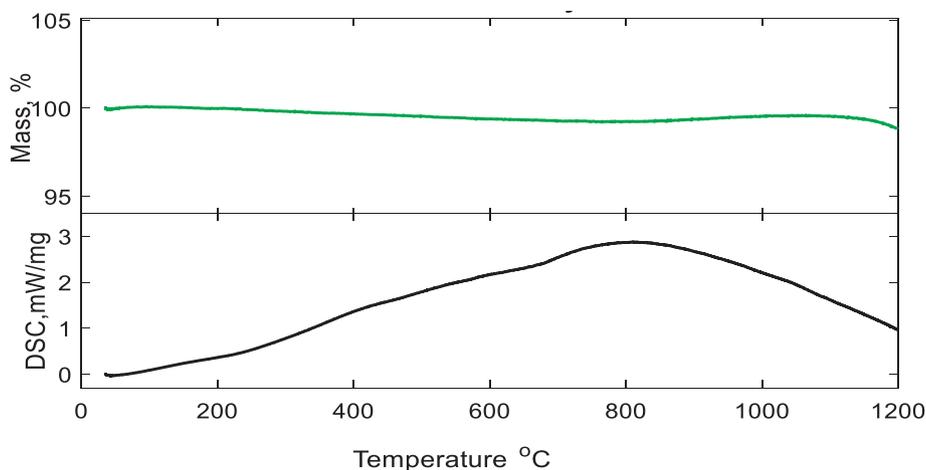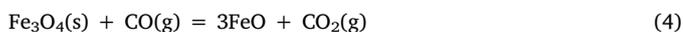
Fig. 4. Thermal analysis of hematite below 1200 °C.

Another mass loss with a corresponding release of CO_2 occurred around 1100 °C. This may be ascribed to the formation of wustite from magnetite as shown in Eq. (4).

Two endothermic peaks were observed during the reduction of hematite using graphite at 1120 °C and 1150 °C respectively as shown in Fig. 9. It is assumed that iron is formed at 1120 °C. This is because at that temperature, there is a steep mass change with a corresponding CO peak. The large change in mass and the formation of high amount of CO indicate the formation of Fe. Jung and Yi (2013) reported the formation of iron from wustite catalyses the gasification of C to CO. The mass change may also be attributed to gasification of carbon or a dominant Boudouard reaction (Eq. (5)). The endothermic peak at 1150 °C is in agreement with the calculated eutectic temperature 1153 °C in the Fe-C system. Furthermore, since iron oxide does not melt in the presence of carbon, at 1150 °C, the DSC peak at that specific temperature under the experimental conditions can only be attributed to the reaction of C with the reduced pure Fe.

$$3Fe_2O_3(s) + C(s) = 2Fe_3O_4(s) + CO(g) \quad (2)$$

$$CO(g) + 3Fe_2O_3(g) = 2Fe_3O_4(s) + CO_2(g) \quad (3)$$

$$Fe_3O_4(s) + CO(g) = 3FeO + CO_2(g) \quad (4)$$

$$C(s) + CO_2(g) = 2CO(g) \quad (5)$$

In the reduction test of hematite with 100%PCB (Fig. 10), the mass

change observed around 300 °C is due to the pyrolysis of the PCB. It can be inferred that the reduction of hematite with PCB starts around 570 °C. This is because, at that temperature, there is a higher change in mass than that of PCB only (Fig. 6). This is confirmed by the release of both CO and CO_2 at that temperature.

The results suggest that the reduction of hematite with PCB (Fig. 10) has faster kinetics than reduction with graphite (Fig. 9). The kinetics of the reduction process was mainly based on the mass lost during the test. Even though both hematite-PCB and hematite-graphite tests were performed using the same heating rate, a higher mass loss slope is observed earlier when PCB is used as reductant. This is because PCB easily releases volatiles which contain hydrocarbons (Fig. 11) capable of reducing hematite at lower temperatures than pure carbon (see Figs. 12–16).

Fig. 11 shows the peaks of CH_4 and C_2H_6 that was detected during hematite-100%PCB blend. The peaks identified at temperatures less than 500 °C is due to the pyrolysis of PCB. The other peaks detected indicates that hydrocarbons are released during the reduction of hematite with PCB or PCB blends which take part in the reduction process as expressed in Eqs. (6) and (7).

The high percentage of volatile matter in PCB increases porosity which facilitates the mass transfer conditions in the gas–solid reaction system and enlarge the reaction interfacial area for reduction which improves reduction of iron oxide.

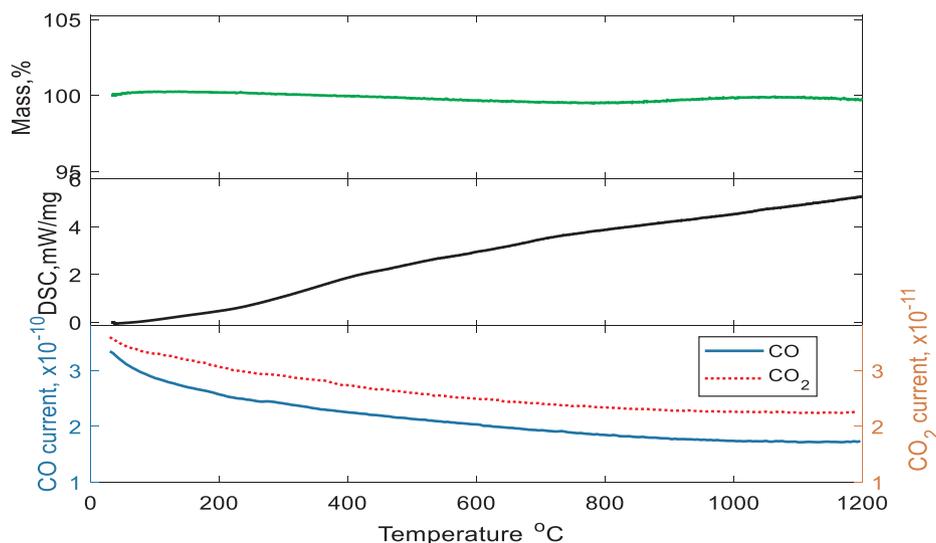As can be seen in Eq. (8), hydrogen takes part in the reduction of

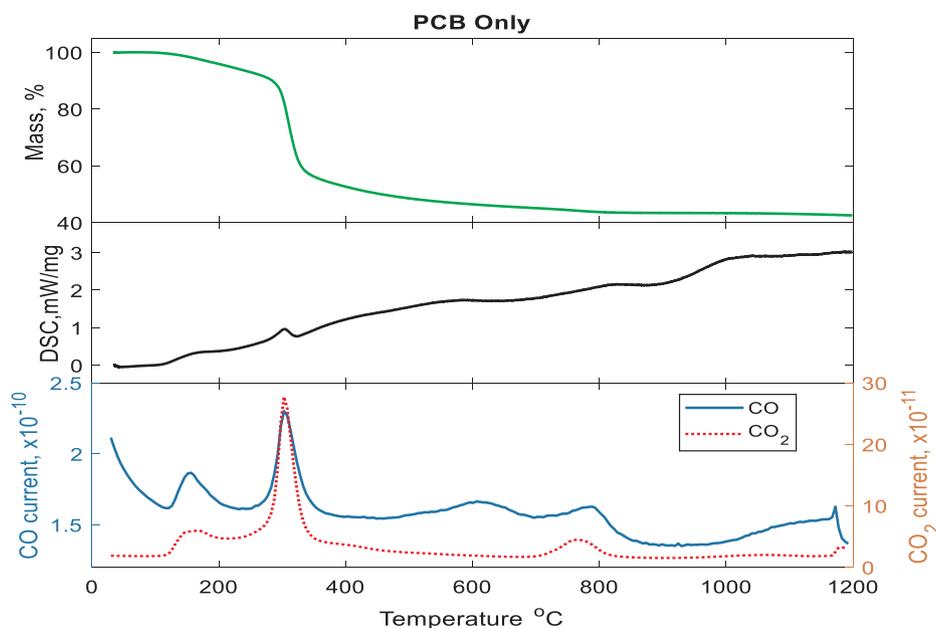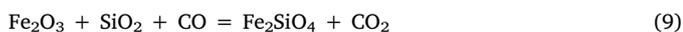**Fig. 5.** Thermal analysis of graphite below 1200 °C.

Fig. 6. Thermal analysis of PCB below 1200 °C.

hematite. Sohn and Fruehan, (2005) reported that up to 900 °C, reduction by H_2 is considerably faster than by carbon in pellet or by CO. Eq. (6) shows the release of hydrogen.

Moreover, it is believed that of plastics content present in the PCB forms a liquid phase which allows it to have more contact with the hematite during reduction experiments (Zhang et al., 2009).

FactSage predicts the formation of fayalite (Fe_2SiO_4) between 200 °C and 800 °C when PCB is used as a reducing agent for hematite. The exothermic peak observed and the release of CO_2 around 750 °C in Fig. 10 may be attributed to the formation of Fe_2SiO_4 (Eq. (9)).

$$Fe_2O_3 + 3CH_4 = 2Fe + 6H_2 + 3CO \qquad (6)$$

$$Fe_2O_3 + 3C_2H_6 = 2Fe + 9H_2 + 3CO \qquad (7)$$

$$Fe_2O_3 + 3H_2 = 2Fe + 3H_2O \qquad (8)$$

$$Fe_2O_3 + SiO_2 + CO = Fe_2SiO_4 + CO_2 \qquad (9)$$

When PCB-graphite blends were used in the reduction of hematite, each test showed the behaviour of both hematite-PCB and hematite-

graphite reductions. Also, it is observed that, as the PCB in the blend used as a reductant increases, the endothermic peak at 1120 °C decreases, even though the shape of the peak becomes more difficult to observe. The decreasing endothermic peak can be ascribed to the decreasing weight percentage of carbon and increasing volatile content in the blend. This observation confirms the results obtained in the mass and energy balance simulations with EMSIM.

3.3. Reduction degree

The reduction degree is related to how much oxygen has been removed from the hematite. The reduction degree was calculated using Eq. (11) based on the mass lost during the reduction in the DSC-TGA (Jung and Yi, 2013).

The overall reduction may be expressed by the reaction

$$Fe_2O_3(s) + 3C = 2Fe + 3CO \qquad (10)$$

$$Reduction\ \ Degree = \frac{\Delta W / W}{3MW_{CO}/(MW_{Fe2O3} + 3MW_C)} \qquad (11)$$
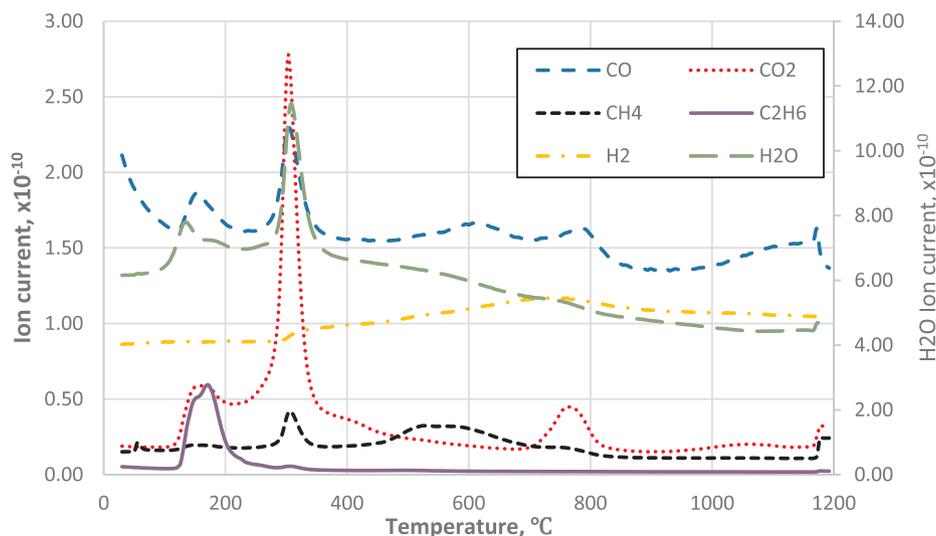

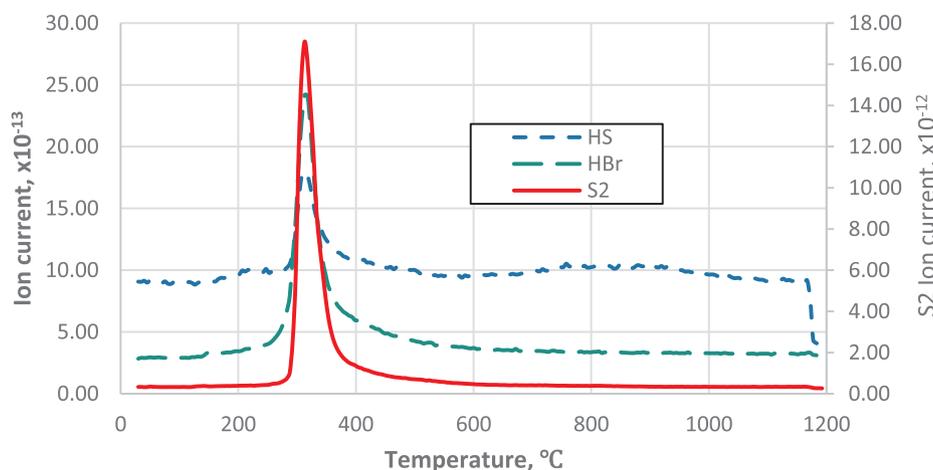**Fig. 7.** Composition of off gas during thermal analysis of PCB.

Fig. 8. Off gases produced with lower ion current.

ΔW = Mass lost; W = initial mass; MW_{CO} = Molecular weight of CO; MW_{Fe2O3} = Molecular weight of Fe_2O_3 and MW_C = Molecular weight of C

The reduction degree calculated revealed PCB reduces hematite better at lower temperatures between 600 °C and 1000 °C. However, at temperatures > 1100 °C, graphite acts as a better reductant. At the end of the reduction test, the use of graphite and 20%PCB gave the highest reduction degree of about 97%. Moreover, it is observed that increasing the mass percent of PCB in the reductant leads to an overall decrease in the reduction degree.

The products obtained from each of the reduction test was analysed using back scattered SEM analysis. The images reveal very bright spots when PCB or blends of PCB are used as reducing agent. SEM produces brighter spots to indicate the presence of elements with higher atomic mass compared to the bulk carbon. The analysis of the bright spots in the products of the reduction with PCB reveal the presence of iron, barium and silicon. The presence of iron and silicon may be attributed to the fayalite that was formed. SEM analysis of hematite-graphite show the presence of only iron and carbon. The image show tiny bright spots which is almost evenly distributed in the sample. This is an indication that the excess carbon melts into the iron that was formed.

3.4. FactSage simulations

Reduction of pure hematite (Fe_2O_3) using pure carbon (graphite) as well as blends of PCB and graphite were simulated using FactSage. This was done to predict and compare the products expected during the reduction test in DSC-TGA. The masses used for the preparation of each sample were used as input in the FactSage and calculations were performed up to 1600 °C with an interval of 25 °C (as described in 2.4). Figs. 17–21 show the mass fraction of the products that were predicted by FactSage.

It can be seen that the formation of solid iron starts around 700 °C for all the reduction tests. Apart from the hematite-100%PCB and hematite-80%PCB reductions, liquid iron in the alloy forms at temperatures above 1150 °C for all the reduction tests. When PCB or blends of PCB are used as reductants, FactSage predicts the formation of fayalite (Fe_2SiO_4) between temperatures 200 °C and 800 °C. This is due to the presence of SiO_2 in the PCB (Eq. (9)). SEM analysis of the product of reduction of hematite with PCB and blends of PCB shows the presence of elements such as iron, silicon and oxygen which indicates the formation of fayalite.

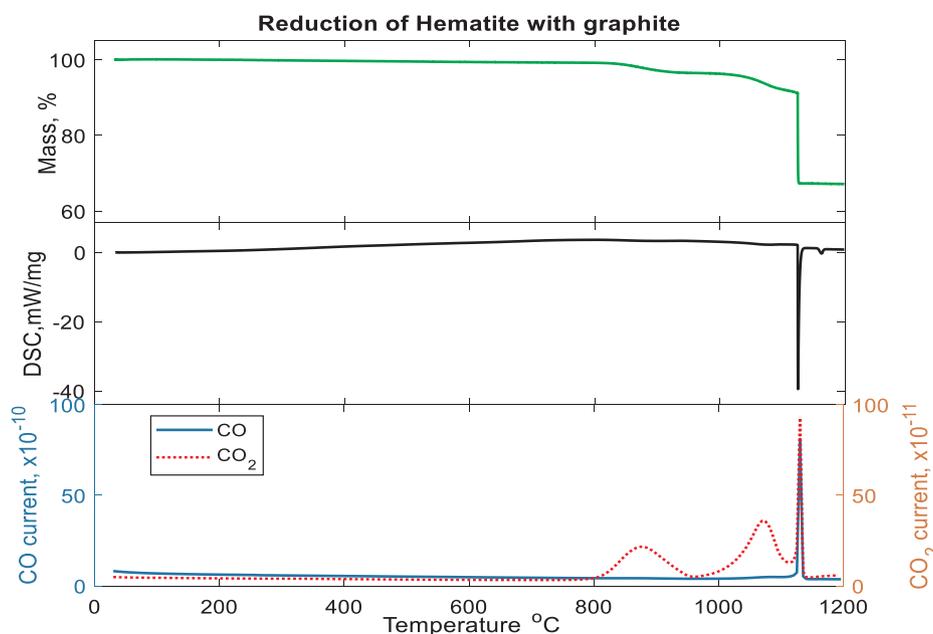At a temperature close to 700 °C, there is a sharp increase in the
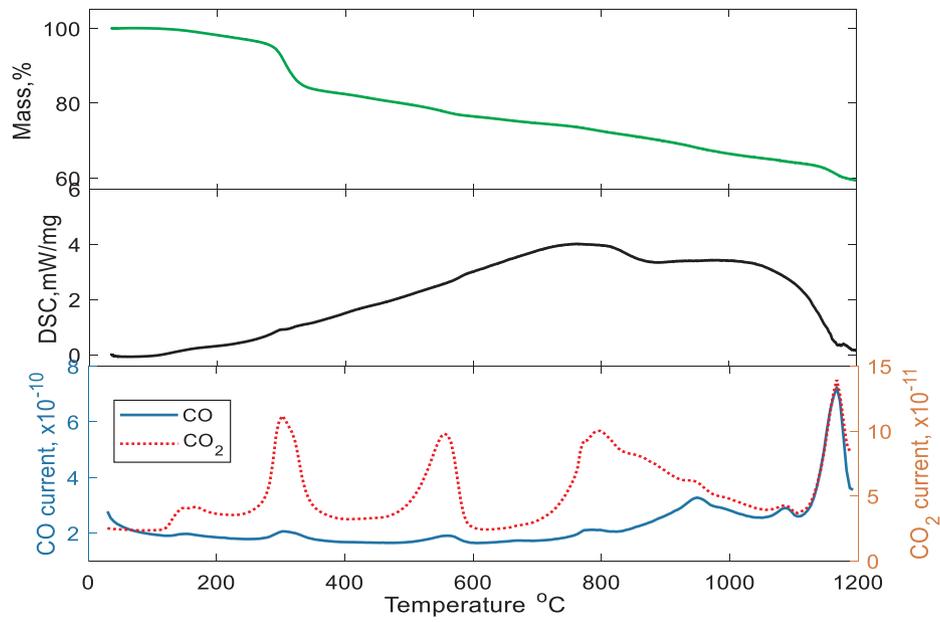

Fig. 9. Reduction of Hematite with Graphite.

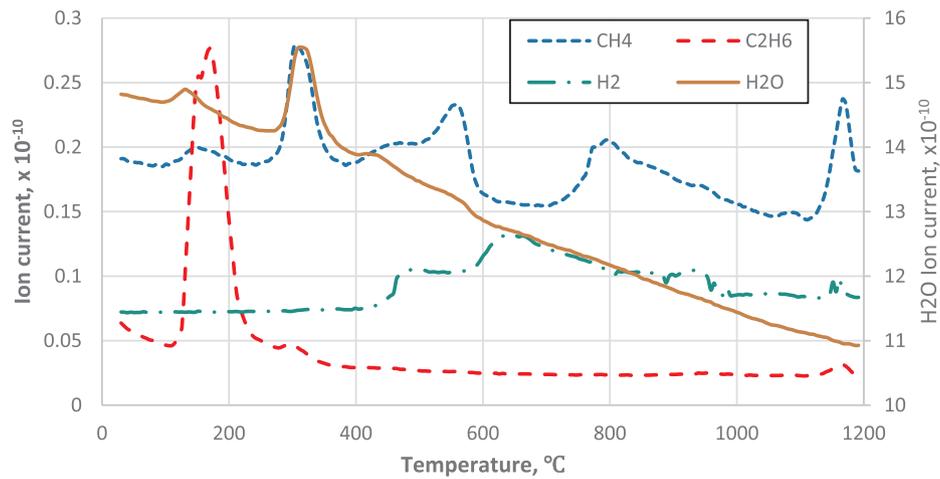**Fig. 10.** Reduction of hematite with 100%PCB.

Fig. 11. Hydrocarbons, H_2O and H_2 present in off-gas during hematite reduction with 100%PCB.
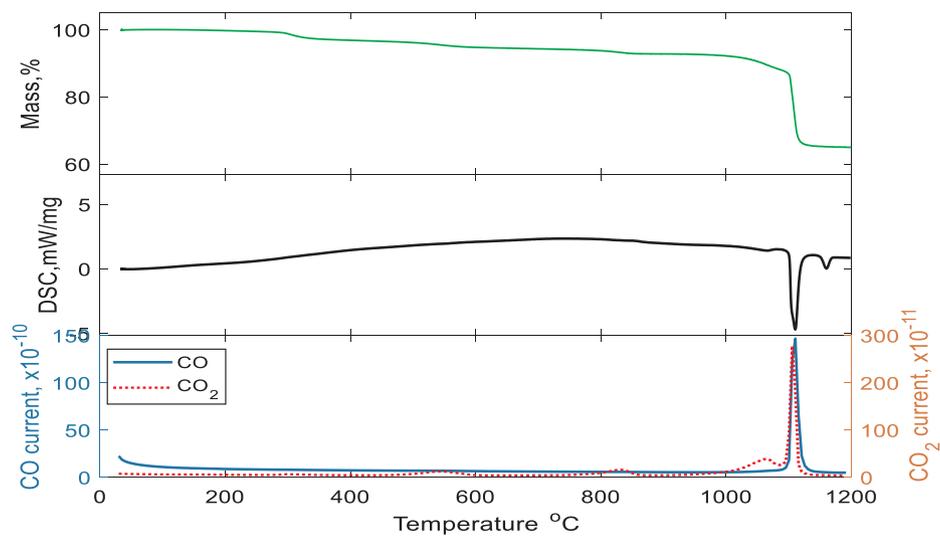

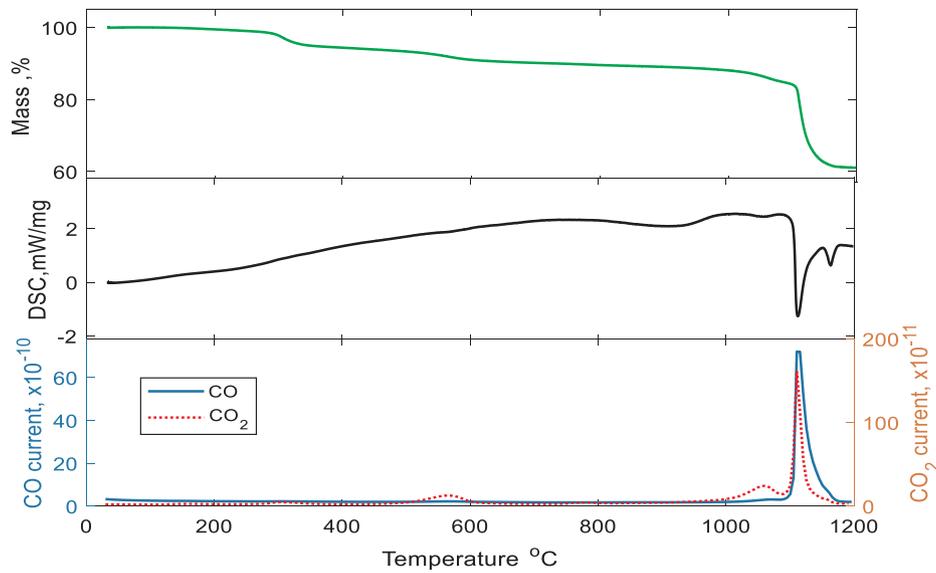**Fig. 12.** Reduction of hematite with 20% PCB.

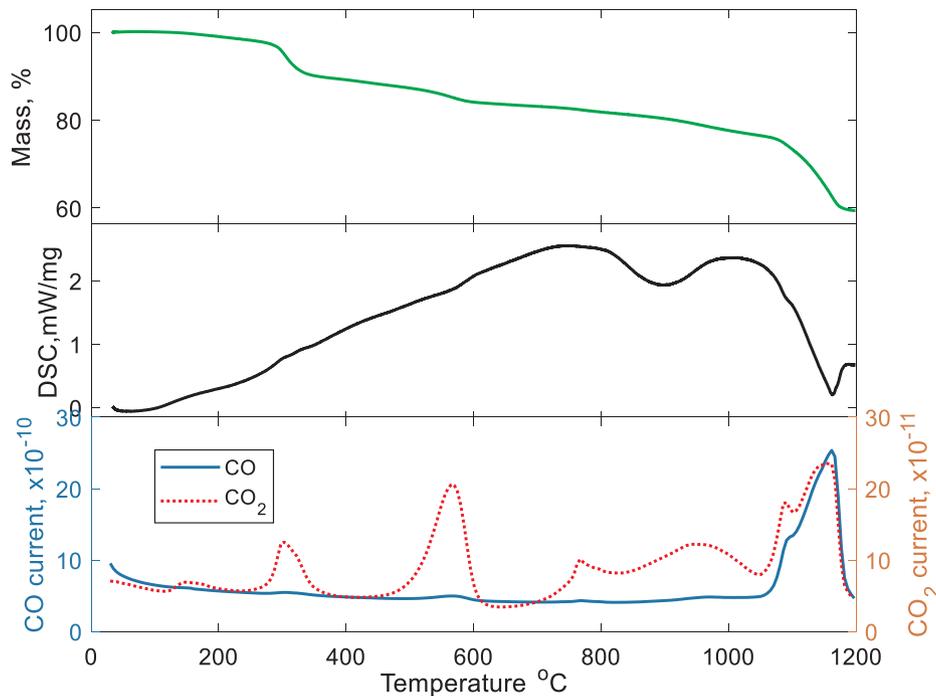**Fig. 13.** Reduction of hematite with 40% PCB.

Fig. 14. Reduction of hematite with 80% PCB.

mass of CO and a decrease in the CO_2 produced. This indicates the gasification of carbon.

Figs. 20 and 21 indicate that all the carbon present in the reductant is used up for hematite-100%PCB and hematite-80%PCB reduction tests.

At temperatures less than 650 °C, FactSage predicts the formation of spinel for all the reduction tests. The spinel consists mainly of Fe_3O_4, with very small quantities of $FeAl_2O_4$ also present when PCB and blends of PCB were used as reducing agents.

The slag predicted by FactSage consists mainly of SiO_2, CaO, and Al_2O_3.

3.5. Iron ore smelting

As shown in Fig. 22, recovery of iron and energy required for the smelting process decreases as the percentage of PCB in the blend increases. It is observed that up to about 20% PCB in the blend, 97% iron was recovered from the ore. 150 kWh less energy was consumed per ton of ore when 20%PCB blend was used as a reductant compared to the usage of coal.

The decrease in the energy required is ascribed to the high percentage of volatile matter present in PCB. Hattori (2005) investigated the use of plastics as reducing agent and observed a reduced electrical power consumption. Zhang et al. (2009) stated that the high volatile matter leads to energy saving and improved efficiency when plastics are used as reducing agents. Moreover, the decrease in metal recovery is ascribed to the lower carbon percentage present in PCB since carbon content is responsible for the reduction of the ore to metal.

During the smelting of iron ore, alloy, gas and slag were obtained as products as shown in Fig. 23. It can be seen that the alloy content
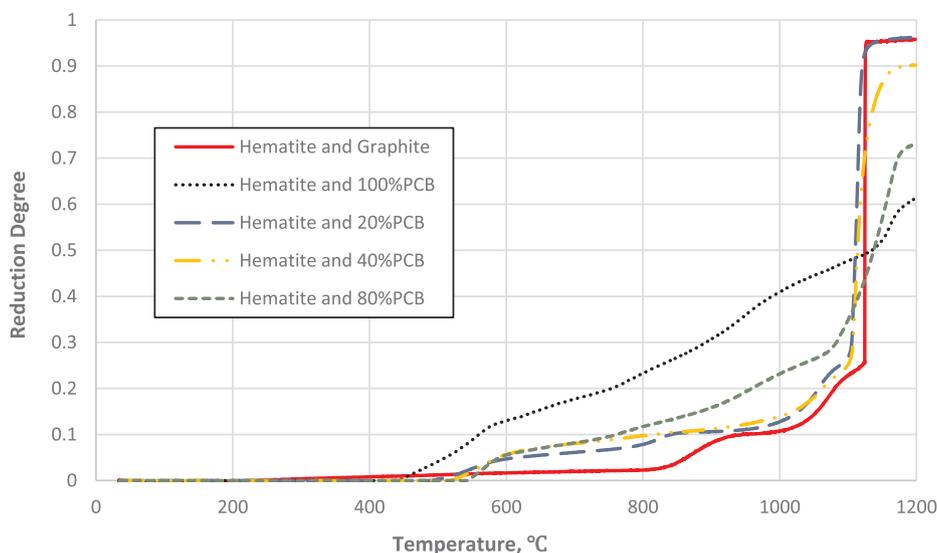
Fig. 15. Reduction degree calculated for the mass lost during test.
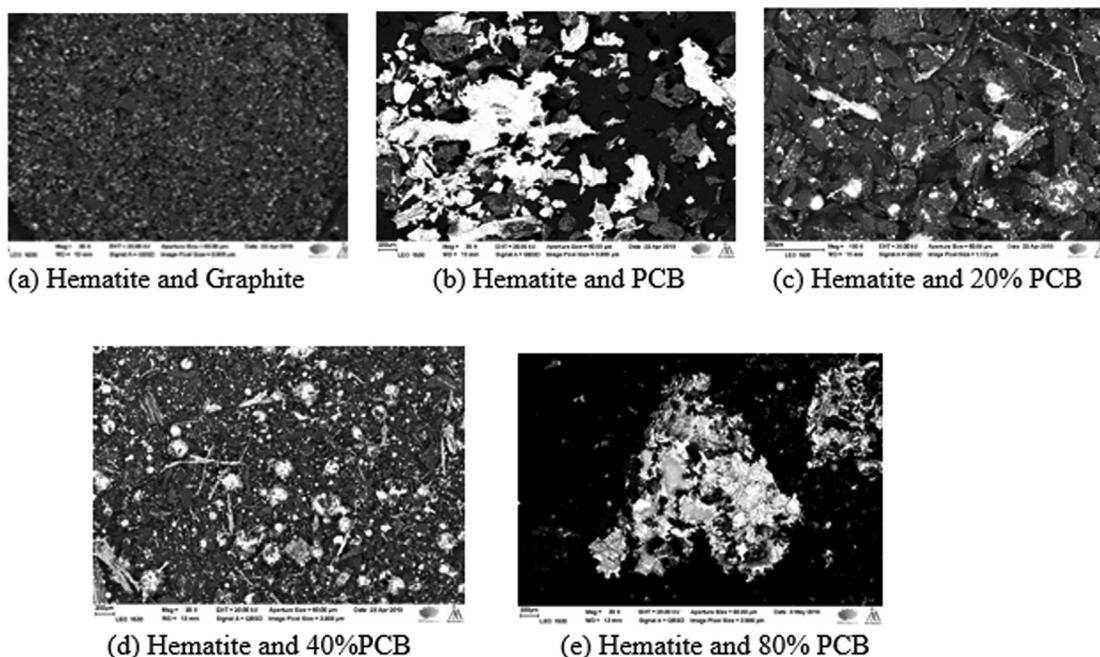

Fig. 16. SEM images of products obtained after reduction of hematite in DSC-TGA.

reduces as the mass percent of PCB increases in the blend (Fig. 24). This is also attributed to the low percentage of carbon in PCB relative to the coal. Sahajwalla et al. (2012) stated that blend of waste plastics and coke can be used to efficiently increase slag foaming in electric arc furnace steelmaking. The results obtained from iron smelting simulation confirmed it because as PCB increases in the blend, the slag formed also increases. This is due to the presence of basic oxides such as CaO, MgO, Fe_2O_3 and the high percentage of SiO_2 present in the PCB. The slag mainly contains SiO_2, Al_2O_3, and MgO.

Since the PCB contains more volatiles, it was expected that the total gas released would be higher during reduction with blends containing higher mass percent of PCB. However, this is not the observation. It can be seen in Fig. 23 that the total gas released decreases as the mass percent of PCB increases in the blend. This is because the volatiles in the PCB contains hydrocarbons which take part in the reduction process.

Fig. 25 shows the mass flowrate of gases that were produced during the smelting of iron. EMSIM predicted that at equilibrium, the composition of the gas include SiO, CH_4, C_2H_2, SiS, etc. These gases were not included in the plot because the individual mass flowrates were less than 0.1 kg/h. It is observed that, in each of the blends, over 80% of the off-gas produced during smelting is CO. Moreover, the flowrate of CO decreases steadily with increase of PCB in the blend. This is an indication of lower carbon unit in the PCB. In addition, the CO_2 flowrate increases as PCB in the blend increases. Dankwah et al. (2015) reported that the use of PET as reducing agent increases the CO_2 produced. The observation in Fig. 25 agrees with their investigation since CO_2 release increased as the mass percent of PCB increases in the blend probably due to the fact that overall CO decreases as reduction decrease leading to higher CO_2 in the gas phase. N_2 released however remained fairly the same around 3 kg/h.

4. Conclusions

The use of printed circuit board leach residue as a reductant in
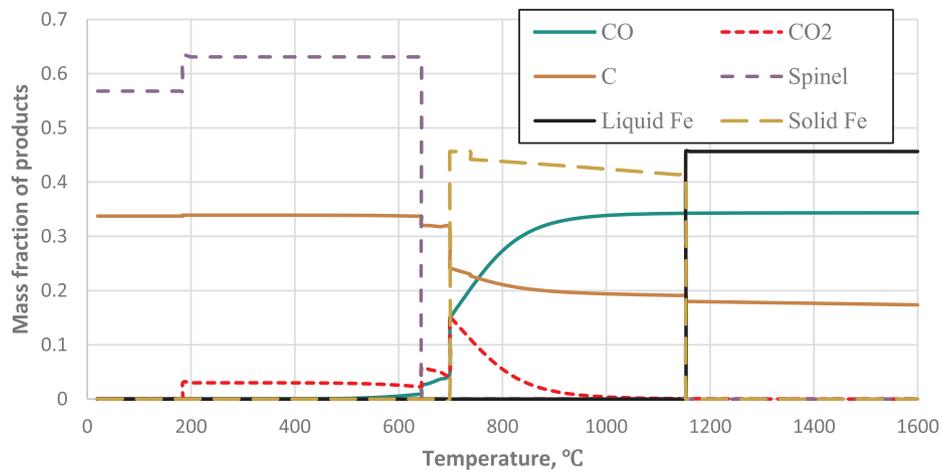
Fig. 17. Mass fraction of products obtained from FactSage calculation during the reduction of hematite with graphite.
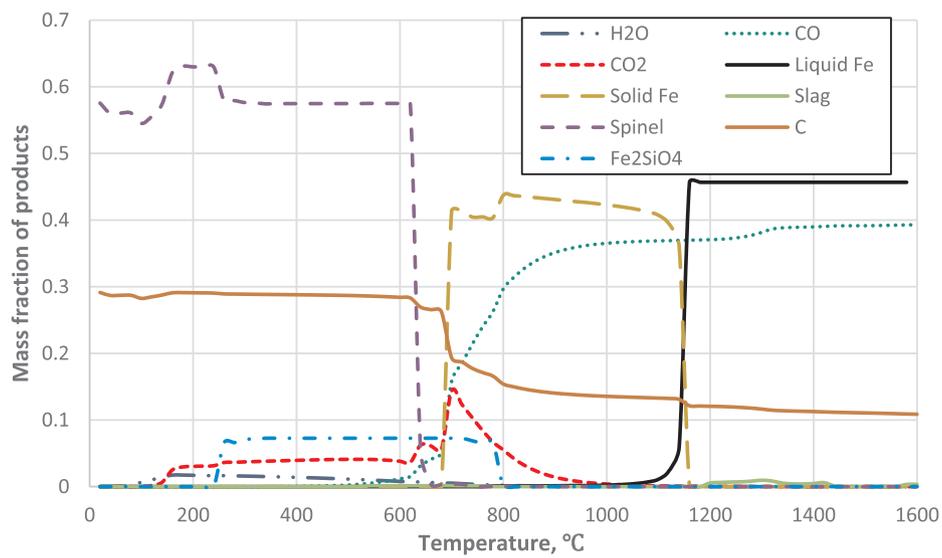

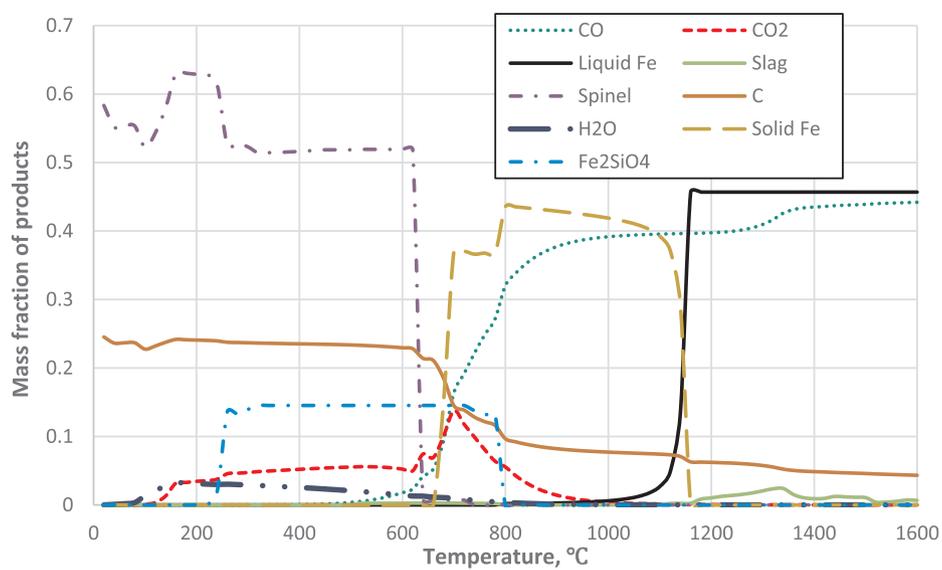**Fig. 18.** Mass fraction of products obtained from FactSage calculation during the reduction of hematite with 20%PCB.

Fig. 19. Mass fraction of products obtained from FactSage calculation during the reduction of hematite with 40% PCB.
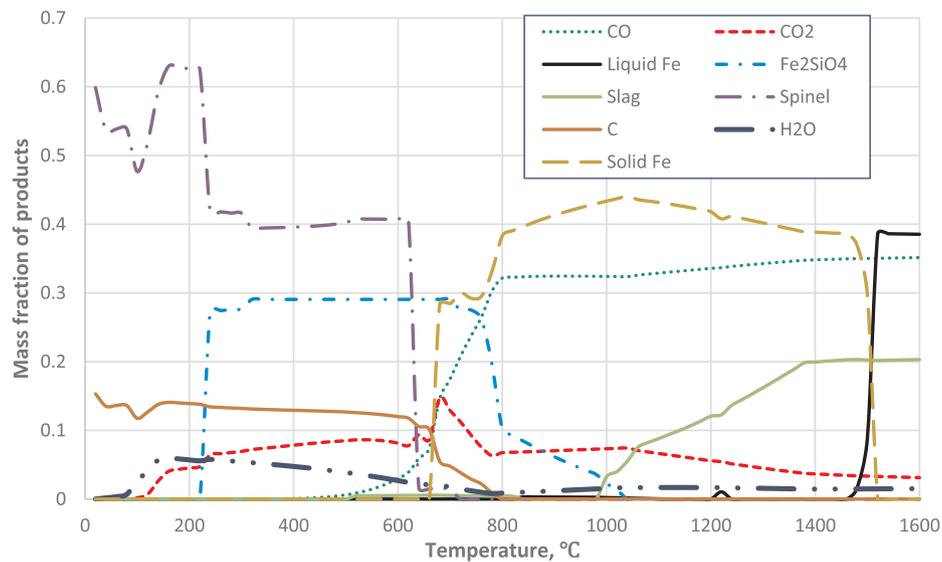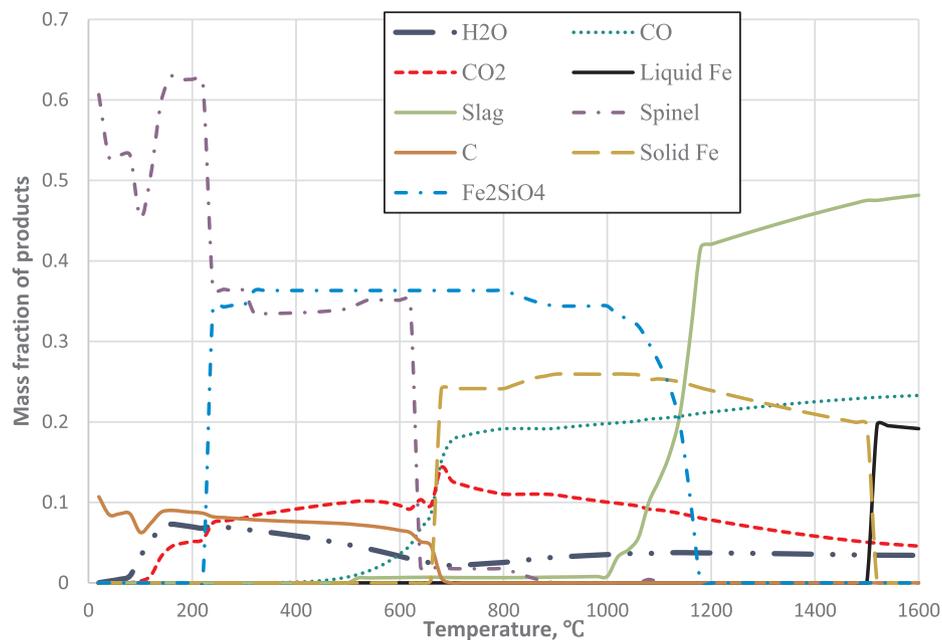
Fig. 20. Mass fraction of products obtained from FactSage calculation during the reduction of hematite with 80%PCB.

Fig. 21. Mass fraction of products obtained from FactSage calculation during the reduction of hematite with 100%PCB.

pyrometallurgy has been investigated using solid-state reduction of hematite in DSC-TGA coupled with QMS and thermodynamic simulations using FactSage and EMSIM software packages. The study revealed that PCB can be used to replace the conventional reducing agents partially. At temperatures below 1000 °C, PCB and blends of PCB with graphite produce a higher reduction efficiency compared to graphite. The high reduction efficiency indicates that PCB is a better reductant at temperatures below 1000 °C. The increased reduction degree is attribute to the presence of hydrocarbons in PCB which take part in the reduction process.

Results observed in this work reveal that when PCB increases in the blend used as reducing agent, the amount of energy required decreases. However, increasing PCB in the blend generally appears to decrease the metal recovery efficiency. Since 150kWh of energy was saved per ton of ore even though a similar metal recovery was attained (97%) with the coal reduction, we consider the optimal PCB blending to be 20%. In the solid-state reduction, 20% PCB in the blend also produces the same reduction degree as pure graphite.

The simulations predict an increase in slag formation when PCB or PCB blends are used as reducing agents which can be attributed to the higher amount of SiO_2 present in PCB.

CRediT authorship contribution statement

Desmond Attah-Kyei: Methodology, Software, Formal analysis, Investigation, Writing - original draft. **Guven Akdogan:** Conceptualization, Supervision, Project administration, Funding acquisition. **Christie Dorfling:** Conceptualization, Methodology, Writing - review & editing, Supervision. **Johan Zietsman:** Software, Resources, Validation. **Daniel Lindberg:** Methodology, Software, Formal analysis, Supervision. **Fiseha Tesfaye:** Resources, Writing - review & editing, Visualization, Funding acquisition. **Quinn Reynolds:** Validation, Resources.
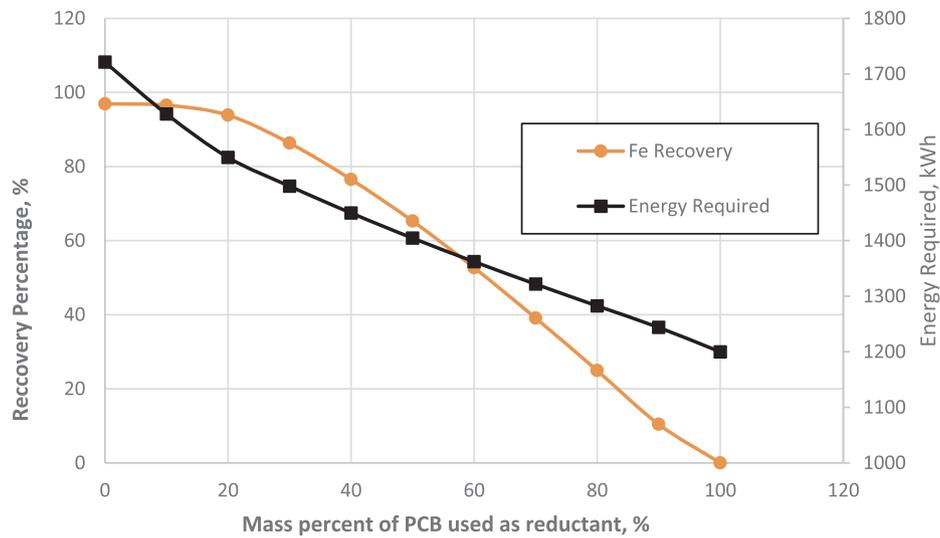
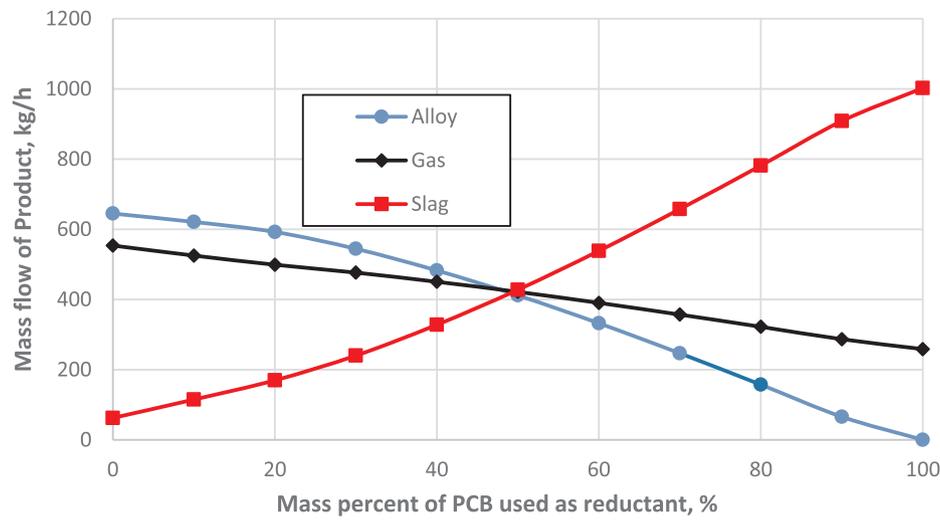**Fig. 22.** Metal recovery and energy required for iron ore smelting.
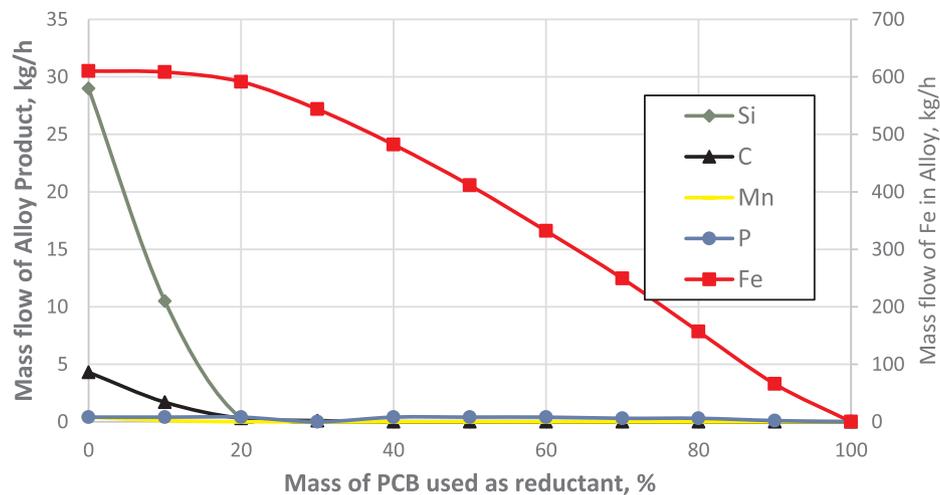

Fig. 23. Products of iron ore smelting.

Fig. 24. Elemental composition of an alloy produced in iron ore smelting.
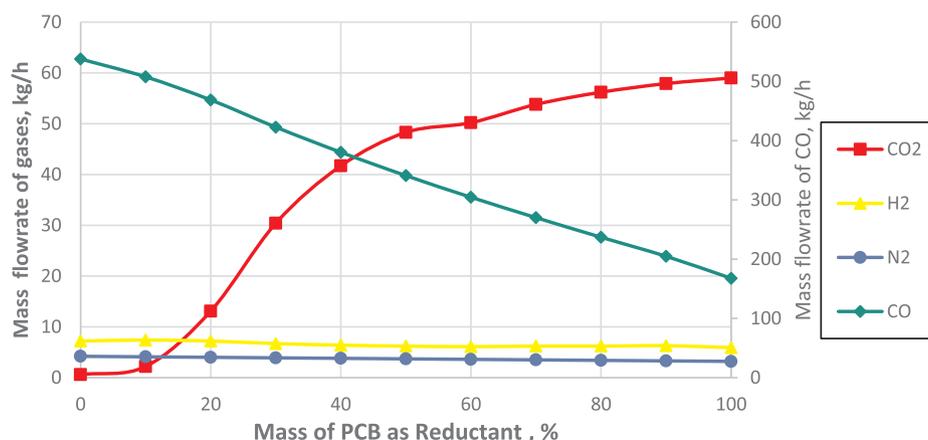
Fig. 25. Mass flow rate of gases produced during iron ore smelting.

Declaration of Competing Interest

The authors declare that they have no known competing financial interests or personal relationships that could have appeared to influence the work reported in this paper.

Acknowledgments

References

Bazargan, A., Bwegendaho, D., Barford, J., McKay, G., 2014. Printed circuit board waste as a source for high purity porous silica. Sep. Purif. Technol. 136, 88–93. https://doi.org/10.1016/j.seppur.2014.08.026.

Cao, X., Prozorov, B., Koltypin, Y., Felner, I., Gedanken, A., 1997. Synthesis of pure amorphous Fe2O3. J. Mater. Res. 2, 2–6.

Carpenter, A.M., 2010. Injection of coal and waste plastics in blast furnaces. Report CCC/166.

Correa, M.M.J., Silvas, F.P.C., Aliprandini, P., de Moraes, V.T., Dreisinger, D., Espinosa, D.C.R., 2018. Separation of copper from a leaching solution of Printed circuit boards by using solvent extraction with D2EHPA. Brazilian J. Chem. Eng. 35, 919–930. https://doi.org/10.1590/0104-6632.20180353s20170144.

Cucchiella, F., D'Adamo, I., Lenny Koh, S.C., Rosa, P., 2015. Recycling of WEEEs: An economic assessment of present and future e-waste streams. Renew. Sustain. Energy Rev. 51, 263–272. https://doi.org/10.1016/j.rser.2015.06.010.

Cui, H., Anderson, C.G., 2016. Literature review of hydrometallurgical recycling of printed circuit boards (PCBs). J. Adv. Chem. Eng. 6, 1–11. https://doi.org/10.4172/2090-4568.1000142.

Cui, J., Zhang, L., 2008. Metallurgical recovery of metals from electronic waste : A review 158, 228–256. https://doi.org/10.1016/j.jhazmat.2008.02.001.

Dankwah, J.R., Amoah, T., Dankwah, J., Fosu, A., 2015. Recycling mixed plastics waste as reductant in ironmaking. Ghana Min. J. 15, 73–80.

Diaz, L.A., Lister, T.E., Parkman, J.A., Clark, G.G., 2016. Comprehensive process for the recovery of value and critical materials from electronic waste. J. Clean. Prod. 125, 236–244. https://doi.org/10.1016/j.jclepro.2016.03.061.

Duan, H., Hou, K., Li, J., Zhu, X., 2011. Examining the technology acceptance for dismantling of waste printed circuit boards in light of recycling and environmental concerns. J. Environ. Manage. https://doi.org/10.1016/j.jenvman.2010.10.057.

Fink, J.K., 1999. Pyrolysis and combustion of polymer wastes in combination with metallurgical processes and the cement industry. J. Anal. Appl. Pyrolysis 51, 239–252. https://doi.org/10.1016/S0165-2370(99)00019-4.

Fisher, M.M., Mark, F.E., Kingsbury, T., Vehlow, J., Yamawaki, T., 2005. Energy Recovery in the Sustainable Recycling of Plastics from End-of-Life Electrical and Electronic Products. Electron. Environ. Proc. 2005 IEEE Int. Symp. 83–92. https://doi.org/10.1109/ISEE.2005.1436999.

Ghosh, B., Ghosh, M.K., Parhi, P., Mukherjee, P.S., Mishra, B.K., 2015. Waste Printed Circuit Boards recycling: An extensive assessment of current status. J. Clean. Prod. 94, 5–19. https://doi.org/10.1016/j.jclepro.2015.02.024.

Guo, Jiuyong, Guo, Jie, Xu, Z., 2009. Recycling of non-metallic fractions from waste printed circuit boards: A review. J. Hazard. Mater. 168, 567–590. https://doi.org/10.1016/j.jhazmat.2009.02.104.

Gurung, M., Adhikari, B.B., Kawakita, H., Ohto, K., Inoue, K., Alam, S., 2013. Recovery of gold and silver from spent mobile phones by means of acidothiourea leaching followed by adsorption using biosorbent prepared from persimmon tannin. Hydrometallurgy 133, 84–93. https://doi.org/10.1016/j.hydromet.2012.12.003.

Hattori, T., 2005. Recycling Technique of Waste Plastics as Carbon Material 50, 27–32.

Hotta, H., 2003. Recycling Technologies for Promoting Recycling-oriented Society Hirohisa. NKK Tech. Rev.

Jung, S.M., Yi, S.H., 2013. A kinetic study on carbothermic reduction of hematite with graphite employing thermogravimetry and quadruple mass spectrometry. Steel Res. Int. 84, 908–916. https://doi.org/10.1002/srin.201200310.

Kleynhans, E.L.J., Beukes, J.P., Van Zyl, P.G., Bunt, J.R., Nkosi, N.S.B., Venter, M., 2017. The effect of carbonaceous reductant selection on chromite pre-reduction. Metall. Mater. Trans. B 48, 827–840. https://doi.org/10.1007/s11663-016-0878-4.

Li, J., Duan, H., Yu, K., Liu, L., Wang, S., 2010. Characteristic of low-temperature pyrolysis of printed circuit boards subjected to various atmosphere. Resour. Conserv. Recycl. 54, 810–815. https://doi.org/10.1016/j.resconrec.2009.12.011.

Nourreddine, M., 2007. Recycling of auto shredder residue 139, 481–490. https://doi.org/10.1016/j.jhazmat.2006.02.054.

Ogunniyi, I.O., Vermaak, M.K.G., Groot, D.R., 2009. Chemical composition and liberation characterization of printed circuit board comminution fines for beneficiation investigations. Waste Manag. 29, 2140–2146. https://doi.org/10.1016/j.wasman.2009.03.004.

Rajagopal, R.R., Rajarao, R., Sahajwalla, V., 2016. High temperature transformations of waste printed circuit boards from computer monitor and CPU: Characterisation of residues and kinetic studies. Waste Manag. 57, 91–101. https://doi.org/10.1016/j.wasman.2015.11.016.

Sahajwalla, V., Zaharia, M., Kongkarat, S., Khanna, R., Rahman, M., Saha-Chaudhury, N., O'Kane, P., Dicker, J., Skidmore, C., Knights, D., 2012. Recycling end-of-life polymers in an electric arc furnace steelmaking process: Fundamentals of polymer reactions with slag and metal. Energy Fuels 26, 58–66. https://doi.org/10.1021/ef201175t.

Shuey, S.A., Taylor, P., 2005. Review of pyrometallurgical treatment of electronic scrap. SME Annual Meeting 1–4. https://doi.org/10.1007/s11837-004-0237-9.

Sohaili, J., Muniyandi, S.K., Mohamad, S.S., 2012. A Review on Printed Circuit Board Recycling Technology Corresponding Author : Johan Sohaili 3, 12–18.

Sohn, I., Fruehan, R.J., 2005. The reduction of iron oxides by volatiles in a rotary hearth furnace process: Part I. The role and kinetics of volatile reduction. Metall. Mater. Trans. B Process Metall. Mater. Process. Sci. 36, 605–612. https://doi.org/10.1007/s11663-005-0051-y.

Stewart, E.S., Lemieux, P.M., 2003. Emissions from the incineration of electronics industry waste. IEEE Int. Symp. Electron. Environ. 2003. https://doi.org/10.1109/ISEE.2003.1208088.

Tesfaye, F., Lindberg, D., Hamuyuni, J., Taskinen, P., Hupa, L., 2017. Improving urban mining practices for optimal recovery of resources from e-waste. Miner. Eng. 111, 209–221. https://doi.org/10.1016/j.mineng.2017.06.018.

Yamane, L.H., de Moraes, V.T., Espinosa, D.C.R., Tenório, J.A.S., 2011. Recycling of WEEE: Characterization of spent printed circuit boards from mobile phones and computers. Waste Manag. 31, 2553–2558. https://doi.org/10.1016/j.wasman.2011.07.006.

Yoo, J.M., Jeong, J., Yoo, K., Lee, J. chun, Kim, W., 2009. Enrichment of the metallic components from waste printed circuit boards by a mechanical separation process using a stamp mill. Waste Manag. 29, 1132–1137. https://doi.org/10.1016/j.wasman.2008.06.035.

Zhang, C., Chen, S., Miao, X., Yuan, H., 2009. Reduction experiment of iron scale by adding waste plastics. J. Environ. Sci. 21, 48–51. https://doi.org/10.1016/S1001-0742(09)60035-8.

Zheng, Y., Shen, Z., Cai, C., Ma, S., Xing, Y., 2009. The reuse of nonmetals recycled from waste printed circuit boards as reinforcing fillers in the polypropylene composites. J. Hazard. Mater. 163, 600–606. https://doi.org/10.1016/j.jhazmat.2008.07.008.

Zie, A., Stanek, W., 2001. Forecasting of the energy effects of injecting plastic wastes into the blast furnace in comparison with other auxiliary fuels 26, 1159–1173.

Zietsman, J.H., Steyn, A., Pretorius, W., 2018. Evaluating Pre-treatment and Smelting Options with EMSIM to Improve Production Efficiency 25–28.